Hindawi
Advances in Meteorology
Volume 2018, Article ID 1419326, 15 pages
https://doi.org/10.1155/2018/1419326

Research Article

Temporal and Spatial Variations of Precipitation $\delta^{18}O$ and Controlling Factors on the Pearl River Basin and Adjacent Regions

Yunfeng Ruan,[1,2] Zhaofei Liu,[1] Zhijun Yao,[1] and Rui Wang[1]

[1] *Institute of Geographic Sciences and Natural Resources Research, Chinese Academy of Sciences, Beijing 100101, China*
[2] *University of Chinese Academy of Sciences, Beijing 100049, China*

Correspondence should be addressed to Rui Wang; wangr@igsnrr.ac.cn

Received 24 September 2017; Revised 15 December 2017; Accepted 31 December 2017; Published 20 February 2018

Academic Editor: Paolo Madonia

Based on the precipitation $\delta^{18}O$ values from the datasets of the Global Network of Isotopes in Precipitation (GNIP), the National Centers for Environmental Prediction/National Center for Atmospheric Research (NCEP/NCAR) Reanalysis data, and previous researches, we explored the temporal and spatial variations of precipitation $\delta^{18}O$ in a typical monsoon climate zone, the Pearl River basin (PRB), and adjacent regions. The results showed that the temporal variations of precipitation $\delta^{18}O$ for stations should be correlated with water vapor sources, the distance of water vapor transport, the changes in location, and intensity of the intertropical convergence zone (ITCZ) rather than "amount effect." Meanwhile, local meteorological and geographical factors showed close correlations with mean weighted precipitation $\delta^{18}O$ values, suggesting that "altitude effect" and local meteorological conditions were significant for the spatial variations of precipitation $\delta^{18}O$. Moreover, we established linear regression models for estimating the mean weighted precipitation $\delta^{18}O$ values, which could better estimate variations in precipitation $\delta^{18}O$ than the Bowen and Wilkinson model in the PRB and adjacent regions.

1. Introduction

Meteoric precipitation is a significant part of the circulation of natural water, and the composition of stable isotopes is closely related to meteorological factors (e.g., temperature, relative humidity, and precipitation amount) and geographical factors (e.g., latitude, altitude, and distance from the moisture transport source), which have shown a sensitive response to environmental change [1–3]. The stable isotopic composition in precipitation can be used as a tracer to reveal the moisture sources [4], retrieve the atmospheric processes [5, 6], and reflect the characteristics of regional climate [7].

Based on the Global Network of Isotopes in Precipitation (GNIP) established by the International Atomic Energy Agency (IAEA) and the World Meteorological Organization, a number of scholars have explored the characteristics of precipitation $\delta^{18}O$ and factors controlling precipitation $\delta^{18}O$ variations [2, 8–10], revealed the original moisture sources of precipitation [11, 12], calculated the contribution ratio of every moisture source to precipitation [9], found significant impacts of climatic events on precipitation $\delta^{18}O$ [13], and utilized models to predict the temporal and spatial distribution of precipitation $\delta^{18}O$ [3, 14–16]. Previous studies have shown that precipitation $\delta^{18}O$ variation for the mid and high-latitude regions is mainly controlled by "temperature effect" and in the low-latitude regions is mainly controlled by "amount effect" [2, 8]. However, not all studies showed "amount effect" in low-latitude regions, but the significance of variation in moisture sources on the precipitation $\delta^{18}O$ variation [17, 18] and different models have represented different simulation accuracy on precipitation $\delta^{18}O$ [3, 14–16]. In China, many studies have explored the temporal and spatial variations of precipitation $\delta^{18}O$ in different geographical zones [15, 16, 19–21], river basins [22–24], and cities [18, 25, 26]. Different moisture sources, which originate from the Arabian Sea, the Bay of Bengal, the South China Sea and the Western Pacific Ocean, and the westerly winds, have remarkable influence on the stable isotopic variations in China

[3, 15, 16]. However, few studies have focused on the Pearl River basin (PRB) and adjacent regions, which have the closer distance to the moisture transport sources for being located in the south of China. This may reveal the more complicated patterns of temporal and spatial distribution of precipitation δ^{18}O and controlling factors. Therefore, this study utilizes precipitation δ^{18}O data from the GNIP and previous studies to (1) understand the temporal and spatial variations of precipitation δ^{18}O in the PRB and adjacent regions; (2) explore the controlling factors on the variation of precipitation δ^{18}O in the PRB and adjacent regions; and (3) establish appropriate spatial models for predicting precipitation δ^{18}O in the PRB and adjacent regions.

2. Study Area, Data, and Methods

2.1. Study Area. The PRB is situated in the south of China, located from 97.65°E to 117.30°E and 3.68°N to 29.25°N. The Pearl River is the second largest Chinese river in terms of streamflow, with a drainage area of 4.42×10^5 km^2 (Pearl River Water Resources Committee (PRWRC), 1991). The mean annual temperature and precipitation range from 14 to 22°C and from 1200 to 2200 mm. In general, the elevation mainly increases from the southeast (southeast delta area) to the northwest (Yunnan–Guizhou Plateau) (Figure 1).

2.2. Data. The precipitation δ^{18}O data in this study mainly come from the GNIP database (http://isohis.iaea.org) and previous studies by Chinese scholars. The stations in the GNIP utilized in this study are Hong Kong (114.17°E, 22.32°N), Guangzhou (113.32°E, 23.13°N), Guilin (110.08°E, 25.07°N), and Liuzhou (109.40°E, 24.35°N) in the PRB and Haikou (110.35°E, 20.03°N), Guiyang (106.72°E, 26.58°N), Kunming (102.68°E, 25.02°N), and Fuzhou (119.28°E, 26.08°N) in the adjacent regions of the PRB. The data included the monthly temperature, precipitation amount, vapor pressure, and precipitation δ^{18}O. Data from previous studies came from the stations of Liangfengdong (108.05°E, 25.27°N) [27], Guilin (110.08°E, 25.07°N) [28], and Huanjiang (108.33°E, 24.74°N) [21] which are located in the PRB, and the stations of Ailaoshan (101.03°E, 24.55°N) [21] and Mengzi (103.23°E, 23.23°N) [30] which are located adjacent to the PRB. The spatial distributions of the stations are shown in Figure 1, and the basic information of sampling stations is shown in Table 1.

2.3. Methods

2.3.1. Precipitation $\delta^{18}O$. All precipitation δ^{18}O data are on a per mil (‰) basis, and δ notation is relative to the Vienna Standard Mean Ocean Water (VSMOW) standard. The δ^{18}O are calculated as follows:

$$\delta^{18}\mathrm{O} = \left(\frac{R_S}{R_{\text{V-SMOW}}} - 1\right) \times 1000, \tag{1}$$

where R_S and $R_{\text{V-SMOW}}$ represent the precipitation samples and R (^{18}O/^{16}O) of VSMOW, respectively.

In this study, the sampling period is divided into the summer monsoon period (May to September), nonsummer monsoon period (October to April), and the annual time scale (January to December).

The mean precipitation δ^{18}O values are the precipitation amount-weighted δ^{18}O values, which are calculated as follows [29]:

$$\overline{\delta^{18}\mathrm{O}} = \sum \delta^{18}\mathrm{O}_i \cdot \frac{P_i}{\sum P_i}, \tag{2}$$

where $\delta^{18}\mathrm{O}_i$ and P_i represent each monthly precipitation δ^{18}O value and the corresponding precipitation amount, respectively.

2.3.2. OLR and Vertically Integrated Moisture Transport. The monthly mean variations of the outgoing longwave radiation (OLR) and vertically integrated moisture transport were adopted from the National Centers for Environmental Prediction/National Center for Atmospheric Research (NCEP/NCAR) Reanalysis data (https://www.esrl.noaa.gov/psd/) during 1980 and 2011.

2.3.3. Linear Correlation Analysis. Monthly precipitation δ^{18}O values for the summer monsoon, nonsummer monsoon periods, and the annual time scale are used to explore the linear correlations with precipitation (mm) and temperature (°C). The correlation is explored for each station alone.

2.3.4. Simulation of the Spatial Distribution of Precipitation $\delta^{18}O$

(1) Nonlinear Regression Model. The Bowen and Wilkinson (BW) model was used as the nonlinear regression model, which was established by Bowen and Wilkinson [14], and has been successfully applied to estimate the spatial distribution of precipitation δ^{18}O [16]. The model considers that the isotopic composition of precipitation is affected by the temperature of driving rainout and the regional patterns of the origin and delivery of moisture. Therefore, the latitude and altitude of the precipitation observation stations are substituted for the temperature effect as the geographic parameters to estimate the isotopic composition of precipitation [14]. The modeled precipitation δ^{18}O has the following form:

$$\delta^{18}\mathrm{O} = a\,|\mathrm{LAT}|^2 + b\,|\mathrm{LAT}| + c\,|\mathrm{ALT}| + d, \tag{3}$$

where δ^{18}O is an observation of the mean weighted value of the oxygen isotopic composition of precipitation and a, b, c, and d are regression parameters. LAT and ALT represent the latitude and altitude, respectively.

(2) Linear Regression Model. Variations in precipitation δ^{18}O are cocontrolled by different meteorological and geographical factors [3, 21, 31]. Meteorological factors in this study come from the China meteorological data sharing service system and include AP, S, WS, P, RH, VP, and T, which represent atmospheric pressure (hPa), sunshine duration (h), wind speed (m/s), precipitation (mm), relative humidity (%), vapor pressure (hPa), and air temperature (°C), respectively, and altitude (m) (ALT) is used as the geographical factor. In

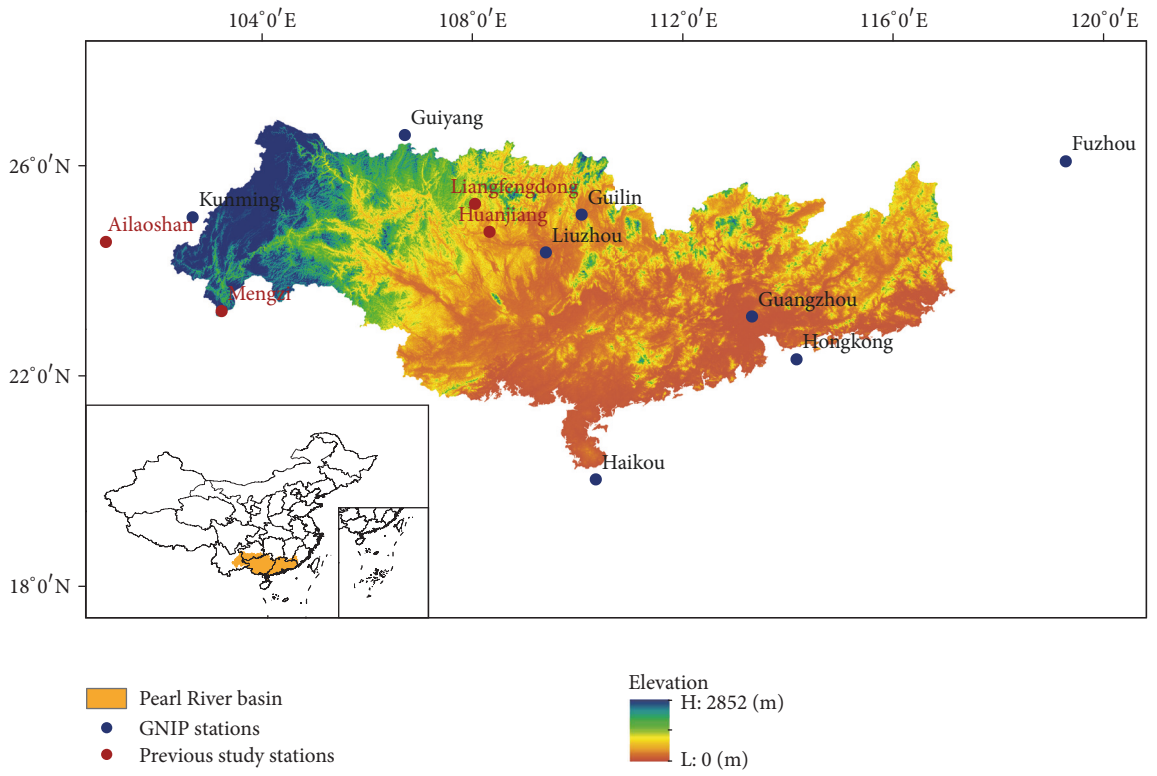

Figure 1: Location of the GNIP and previous studies stations in the PRB and adjacent regions.

Table 1: Basic information of sampling stations.

Sample site	Latitude (°N)	Longitude (°E)	Altitude (m)	Study periods	Data sources
Hong Kong	22.32	114.17	66	1961–2014	GNIP
Haikou	20.03	110.35	15	1988–2000	GNIP
Guangzhou	23.13	113.32	7	1986–1989	GNIP
Guilin	25.07	110.08	170	1983–1990	GNIP
Guilin	25.07	110.08	170	2010	Wu et al. [28]
Liuzhou	24.35	109.40	97	1988–1992	GNIP
Guiyang	26.58	106.72	1071	1988–1992	GNIP
Kunming	25.02	102.68	1892	1986–2003	GNIP
Fuzhou	26.08	119.28	16	1985–1992	GNIP
Liangfengdong	25.27	108.05	620	2003-4~2003-9, 2004-3~2004-5	Luo et al. [27]
Huanjiang	24.74	108.33	400	2005–2010	Liu et al. [21]
Ailaoshan	24.55	101.03	2481	2005–2010	Liu et al. [21]
Mengzi	23.23	103.23	1302	2009–2011	Li et al. [30]

order to compare the factors controlling precipitation δ^{18}O values among stations under different time scales in the PRB and adjacent regions, linear correlations between the mean weighted precipitation δ^{18}O values of all stations and their corresponding mean meteorological values and altitude were calculated on the three time periods, while stations of Liangfengdong, Huanjiang, Ailaoshan, and Mengzi were only calculated for the annual time scale.

The modeled precipitation δ^{18}O has the following form:

$$\delta^{18}\mathrm{O} = aX1 + bX2 + cX3 + \cdots + nXn, \quad (4)$$

where δ^{18}O is an observation of the mean weighted value of the oxygen isotopic composition of precipitation, $X1, X2, X3, \ldots, nXn$ represent different meteorological and geographical factors that are correlated with the mean weighted precipitation δ^{18}O value at P value < 0.05 or 0.01, and $a, b, c, \ldots, n$ are regression parameters.

3. Results and Discussion

3.1. Correlations of Precipitation δ^{18}O for Stations with Temperature and Precipitation Amount. The positive correlation

Table 2: Correlations of monthly precipitation $\delta^{18}O$ values at different stations with precipitation amount and temperature for three time periods in different stations of the PRB and adjacent regions. Note: $*$ and $**$ are represent the correlations at P values < 0.01 and 0.05, respectively. The units of $d\delta^{18}O/dP$ and $d\delta^{18}O/dT$ are 100 mm and 1°C, respectively.

	Station	Precipitation amount		Temperature	
		$r_{\delta\text{-}P}$	$d\delta^{18}O/dP$	$r_{\delta\text{-}T}$	$d\delta^{18}O/dT$
Summer monsoon period	Haikou	0.10	0.17	−0.47**	−1.02
	Hong Kong	−0.29**	−0.27	−0.24**	−0.38
	Guangzhou	−0.28	−0.41	−0.13	−0.26
	Guilin	0.26	0.44	−0.32*	−0.34
	Liuzhou	−0.07	−0.12	−0.27	−0.23
	Guiyang	−0.25	−1.08	−0.32	−0.50
	Kunming	−0.37**	−1.28	0.09	0.03
	Fuzhou	−0.59**	−1.09	0.19	0.14
Nonsummer monsoon period	Haikou	−0.18	−0.41	−0.37	−0.26
	Hong Kong	−0.42**	−0.21	−0.34**	−0.21
	Guangzhou	−0.25	−0.68	−0.38	−0.24
	Guilin	0.11	0.32	−0.34**	−0.16
	Liuzhou	−0.12	−0.71	−0.35	0.00
	Guiyang	−0.36*	−3.26	−0.31	−0.20
	Kunming	−0.67**	−7.15	−0.12	0.06
	Fuzhou	0.02	0.05	−0.29	−0.21
The annual time scale	Haikou	−0.20	−0.43	−0.65**	−0.50
	Hong Kong	−0.61**	−0.92	−0.67**	−0.38
	Guangzhou	−0.44**	−0.80	−0.50**	−0.84
	Guilin	−0.17*	−0.45	−0.71**	−0.29
	Liuzhou	−0.33*	−1.34	−0.60**	−0.26
	Guiyang	−0.48**	−2.46	−0.57**	−0.28
	Kunming	−0.62**	−4.37	−0.44**	−0.53
	Fuzhou	−0.35**	−0.89	−0.38**	−0.16

between isotopic composition and temperature was called "temperature effect," while negative correlation between isotopic composition and precipitation amount was called "amount effect" [8, 32]. The correlations between monthly precipitation $\delta^{18}O$ of each station and precipitation amount, temperature, and the slopes $d\delta^{18}O_p/dP$ and $d\delta^{18}O_p/dT$ are shown in Table 2. Precipitation $\delta^{18}O$ shows significant negative correlations with temperature in all stations under the annual time scale and in partial stations under the summer monsoon and nonsummer monsoon periods, which shows opposite result to the "temperature effect" of precipitation $\delta^{18}O$, suggesting the "temperature effect" is rarely found in the summer monsoon areas with low latitudes but mainly occurs in mid-high latitudes, especially near the poles [32], and in nonsummer monsoon areas [11]. Except for Haikou under the annual time scale, precipitation $\delta^{18}O$ has stronger negative correlations with the precipitation amount, especially at the stations of Hong Kong and Kunming, with correlation coefficients of −0.61 and −0.62 and P values < 0.01 and 0.01, respectively, which suggests that precipitation $\delta^{18}O$ is significantly influenced by the "amount effect" in the monsoon regions [3, 8]. However, only three stations have correlations with the precipitation amount under the summer monsoon and nonsummer monsoon periods, suggesting the "amount effect" mainly occurs under the annual time scale. Except for Fuzhou under the summer monsoon period, the slopes of $d\delta^{18}O_p/dP$ for Guiyang and Kunming are significantly higher than other stations in the PRB and adjacent regions (Table 2), and stations of $r_{\delta\text{-}P}$ at P value < 0.05 or 0.01 for the annual time scale show significant correlations (P value < 0.01) with altitude (Figure 2). This is mainly because the higher altitude areas experience greater temperature drop for wet air-parcels as the decrease in absolute humidity, resulting in greater slopes of $d\delta^{18}O_p/dP$ [2].

3.2. Precipitation $\delta^{18}O$ Variations at Stations in the PRB and Adjacent Regions. The mean monthly precipitation amount, air temperature, and mean weighted precipitation $\delta^{18}O$ values in the sampling period for each precipitation station of the GNIP are shown in Figure 3. The precipitation $\delta^{18}O$ values present "V-shaped" patterns in all stations, which show a decreasing trend as the temperature and the precipitation amount increase and an increasing trend as the temperature and the precipitation amount decrease (Figure 3). Precipitation $\delta^{18}O$ values at the stations show significant seasonal variation, with more depleted mean precipitation $\delta^{18}O$ values in the summer monsoon period and more enriched $\delta^{18}O$ values in the nonmonsoon period (Figure 3). Our results reveal significantly negative correlation between precipitation $\delta^{18}O$

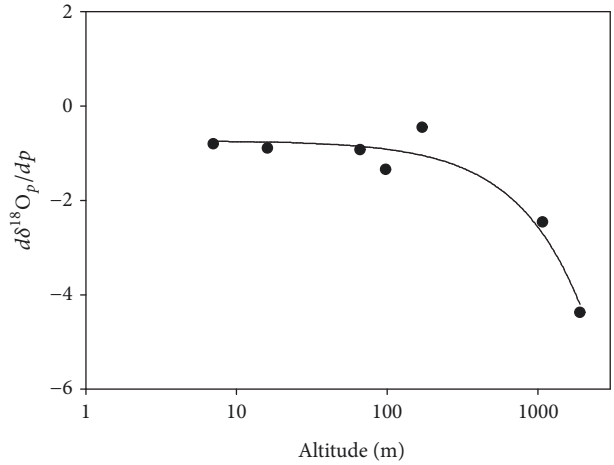

Figure 2: Correlations of $d\delta^{18}O_p/dP$ ($r_{\delta\text{-}P}$ at a P value < 0.05 or 0.01) with altitude for the annual time scale.

values for each station and precipitation amount in the annual time scale (Table 2), which shows "amount effect" for each station. However, the most depleted precipitation $\delta^{18}O$ value for each station does not occur in the month with the most precipitation amount. This phenomenon has also been observed in other monsoon regions [18, 21, 33, 34]. Mean weighted precipitation $\delta^{18}O$ values (the annual time scale, the summer monsoon, and the nonsummer monsoon periods) are more enriched at the stations of Guangzhou (−5.83‰, −6.27‰, and −4.09%), Haikou (−6.09‰, −7.80‰, and −4.12‰), Hong Kong (−6.59‰, −7.16‰, and −4.09‰), Liuzhou (−6.37‰, −8.09‰ and, −3.74‰), Guilin (−6.12‰, −7.76‰, and −3.56‰), Fuzhou (−6.6‰, −7.73‰, and −4.44‰), and Huanjiang (−6.16‰) with the lower altitude comparison with the more depleted values at the stations of Guiyang (−8.32‰, −9.42‰, and −5.55‰), Kunming (−10.11‰, −10.67‰, and −8.00‰), Liangfengdong (−7.3‰), Mengzi (−7.26‰), and Ailaoshan (−9.22‰) with higher altitude (Huanjiang, Liangfengdong, Mengzi, and Ailaoshan do not have the mean weighted values for the summer monsoon and nonsummer monsoon periods), suggesting differences in spatial distribution characteristics of precipitation $\delta^{18}O$. By comparing these values with the mean annual precipitation amount Figure 3, the result shows that the most depleted mean annual precipitation $\delta^{18}O$ values do not occur in the station with the most mean annual precipitation amount. Both of the seasonal and spatial characteristics of variations show that there exist other factors controlling the precipitation $\delta^{18}O$ variations rather than "amount effect."

3.3. Controlling Factors on the Precipitation $\delta^{18}O$ Variation

3.3.1. Effects of Changes in Water Vapor Sources and Vapor Transport on Seasonal Precipitation $\delta^{18}O$ Variation. Water vapor sources and vapor transport influence significantly the precipitation $\delta^{18}O$ variations [3, 15, 16, 18, 31]. The intertropical convergence zone (ITCZ) is a major convergence zone of the troposphere wind field that always closely tracks with monsoon activity and moisture source for precipitation [18]. Outgoing long wave radiation (OLR) is closely related to convection activities, with low OLR values reflecting strong convection activities, conversely, reflecting weak convection activities. The distribution area of low OLR values can accurately reflect the location and intensity changes of the ITCZ to reveal the moisture sources for the summer monsoon precipitation [35]. Therefore, the average OLR values for each month from 1980 to 2011 were calculated (Figure 4). In addition, the average vertically integrated moisture transport for each month from 1980 to 2011 which was calculated by multiplying the zonal and meridional winds by specific humidity from the surface to the 300 hPa level (Figure 5) was used to explore the effects of changes in moisture sources and vapor transport on precipitation $\delta^{18}O$.

In spring, the ITCZ is mainly distributed near the equator regions in March and April, with a weak intensity in the ITCZ and a long distance from the water vapor sources to the PRB and adjacent regions (Figure 4). The PRB and adjacent regions are dominated by a westerly system, with a small water vapor transport (Figure 5), resulting in enriched precipitation $\delta^{18}O$ (Figure 3) contributed by local evaporation and inland evaporation taken by the westerly system. In May, the ITCZ gradually moves to the Bay of Bengal, with a strengthening in the intensity of the ITCZ that suggests the onset of the Asian summer monsoon (Figure 4). The prevailing wind direction gradually shifts from a westerly system to a south wind (Figure 5). Large amounts of moisture are brought from the Bay of Bengal and strong convection occurs in the water vapor sources. The vapor transportation depletes the $\delta^{18}O$ in water vapor, which causes the shape decrease in the precipitation $\delta^{18}O$ for May in comparison to April (Figure 3).

In summer, the convection center of the ITCZ moves further to the north with the rapidly strengthening intensity in the Bay of Bengal, the South China Sea, and the Arabian Sea in June (Figure 4), and the prevailing wind direction is dominated by a southwest wind (Figure 5). As large amounts of moisture are brought to the PRB and adjacent regions by the southwest wind, a stronger convection occurs in the water

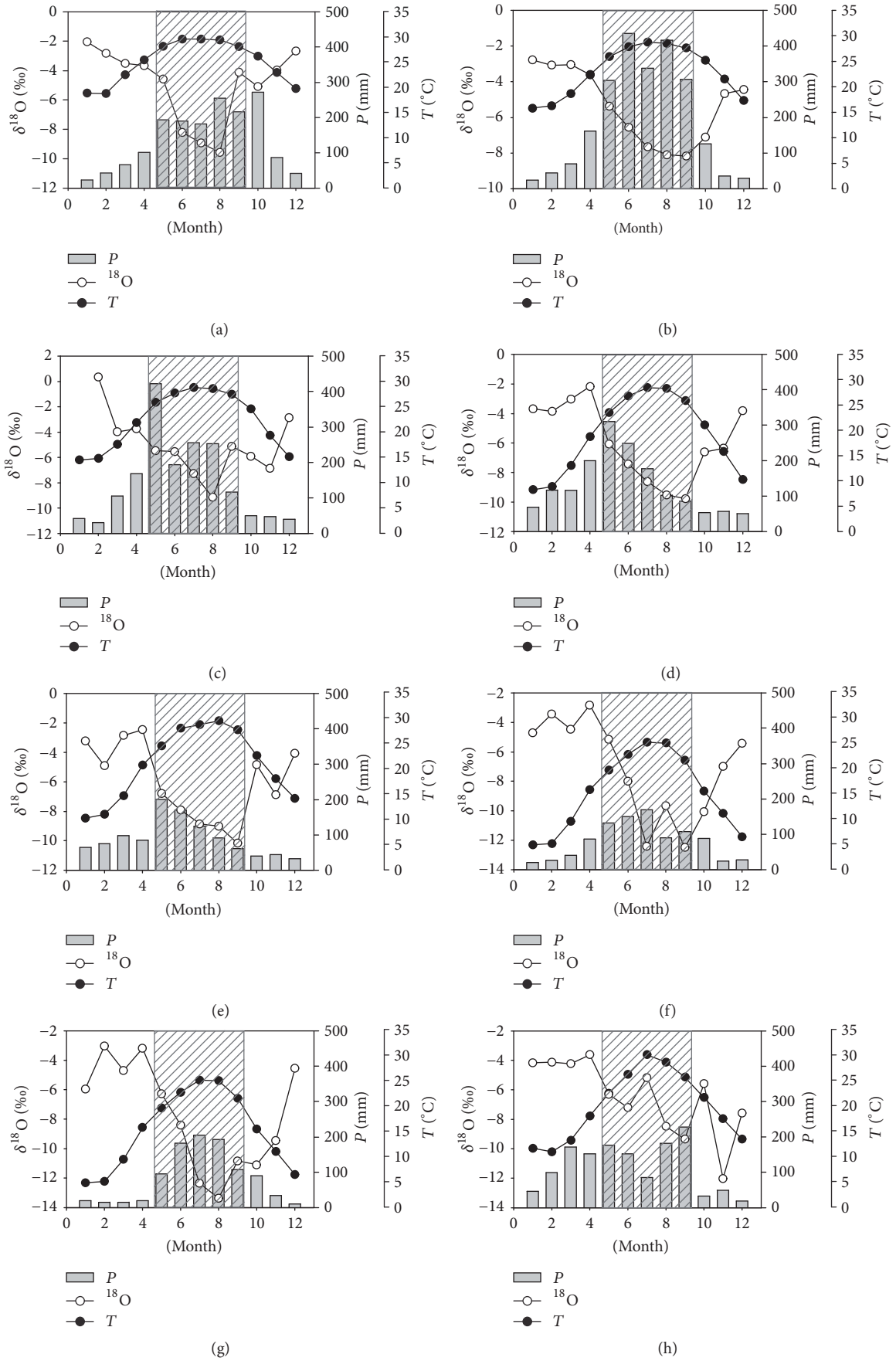

Figure 3: Variations of mean monthly weighted precipitation $\delta^{18}O$, temperature, and precipitation amount at Haikou (a), Hong Kong (b), Guangzhou (c), Guilin (d), and Liuzhou (e) stations in the PRB and at Guiyang (f), Kunming (g), and Fuzhou (h) adjacent to the PRB. Note: the shadow area represents the monsoon period (May to September).

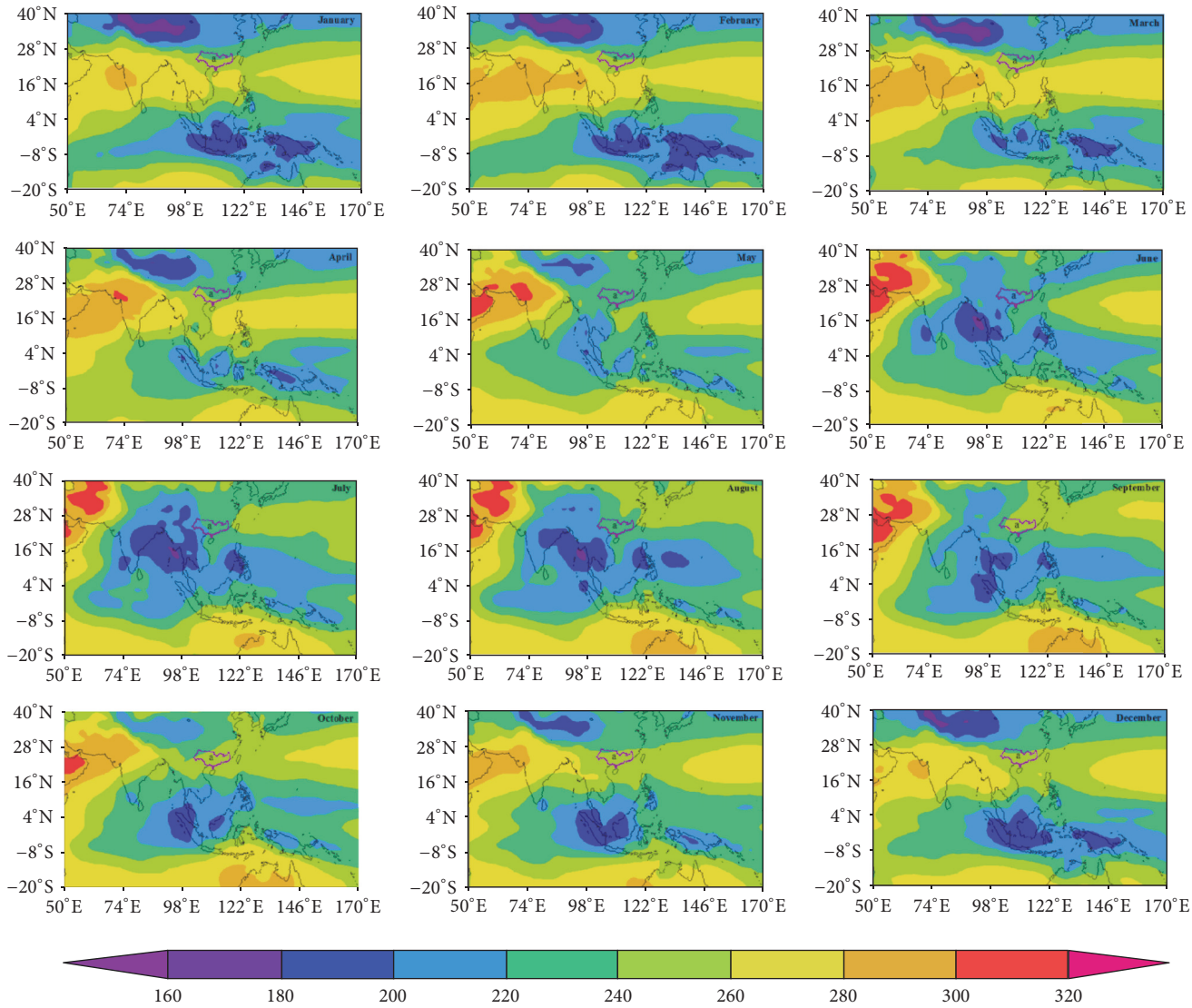

Figure 4: Variations of mean OLR for each month from 1980 to 2011 over Pearl River basin (a) and adjacent regions. Note: the unit of the color scale is W/m^2.

vapor sources and vapor transportation, resulting in a continuous decrease in the precipitation δ^{18}O in the PRB and adjacent regions. In July, the prevailing wind direction and water vapor transport do not change too much compared with that in June, but the strong intensity convention for the ITCZ is enlarged further in the Bay of Bengal and the Indo-China Peninsula, depleting the δ^{18}O in the water vapor and continuously decreasing the precipitation δ^{18}O in the PRB and adjacent regions. In August, by comparison with July, the prevailing wind direction in the PRB and adjacent regions becomes jointly controlled by southwest and southeast winds (Figure 5). The scope of the convection in the ITCZ is narrowed in the Bay of Bengal, but the intensity of the convection increases in the western Pacific Ocean (Figure 4), which increases the distance for water vapor transport to the PRB and adjacent regions. These changes contribute to the depleted precipitation δ^{18}O values in the PRB and adjacent regions (Figure 3).

In autumn, the prevailing wind direction does not change much in September as compared with August (Figure 5). However, the convective centers of the ITCZ in the Bay of Bengal and the South China Sea move southward (Figure 4), which increases the distance for water vapor transport to the PRB and adjacent regions. As a result, the stations experience decreasing precipitation δ^{18}O values, with Guilin and Liuzhou obviously reaching their most depleted precipitation δ^{18}O values during this month. However, Haikou and Guangzhou do not reach their most depleted precipitation δ^{18}O values in September but have significantly higher values than the most depleted values obtained in August (Figure 3). As shown in Figure 5, the water vapor sources originate from the Bay of Bengal and South China Sea and also originate from the adjacent seas in September. Moreover, Haikou and Guangzhou are all coastal stations in the south of PRB, which results in higher precipitation δ^{18}O values than in August due to the relatively shorter distance for water vapor transport.

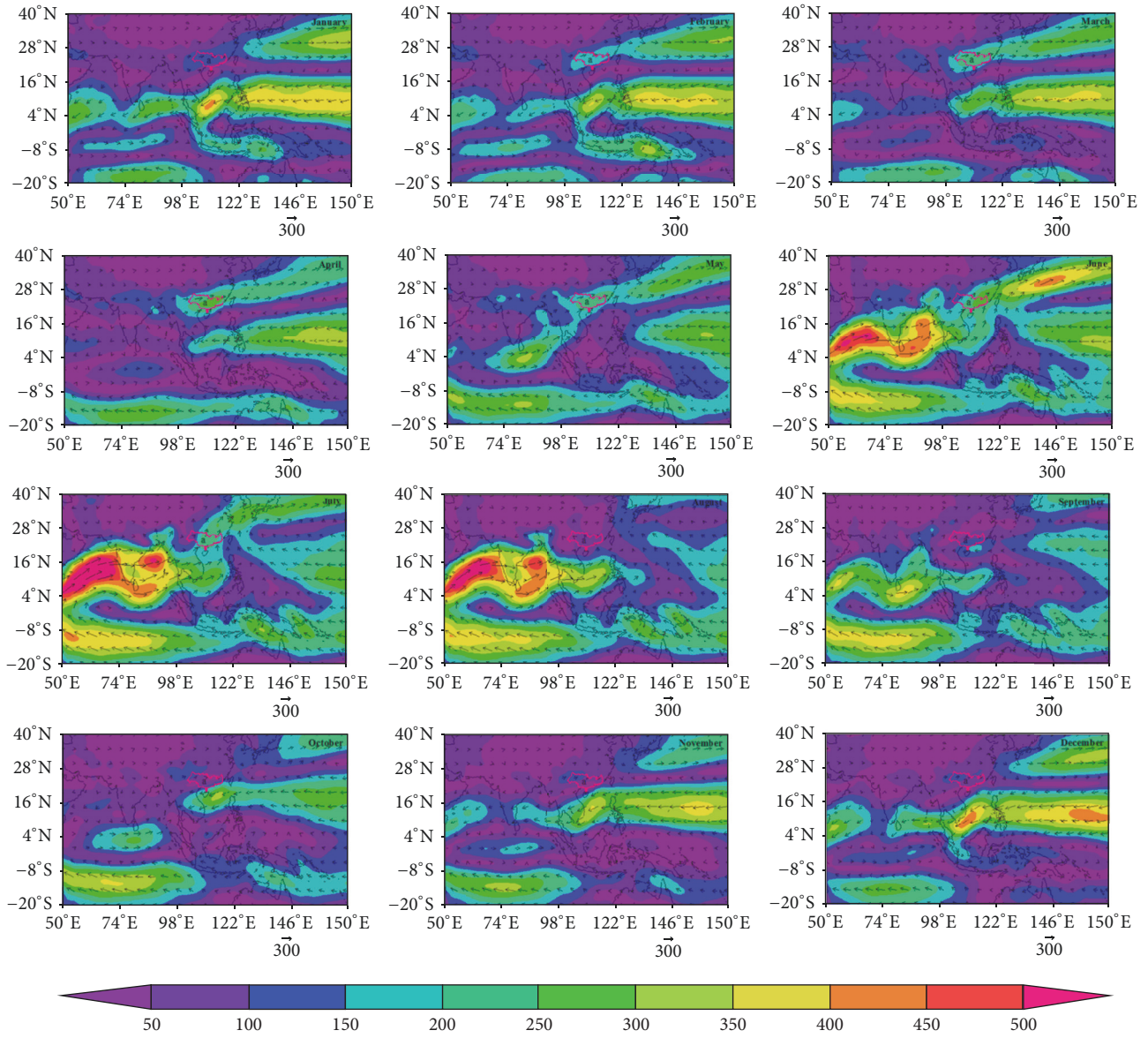

Figure 5: Vertically integrated mean moisture transport (kg m^{-1} s^{-1}) for each month from 1980 to 2011 over Pearl River basin (a) and adjacent regions. Note: the unit of the color scale is kg m^{-1} s^{-1}.

From October to November, the prevailing wind direction changes from southwest and southeast to west, and the ITCZ moves further southward to the vicinity of the equator, suggesting that the summer monsoon has disappeared. The water vapor sources mainly originate from the inland [3], resulting in enriched precipitation δ^{18}O values in the PRB and adjacent regions (Figure 3).

In winter, water vapor mainly originates from local evaporation and inland evaporation due to the westerly system (Figure 5), resulting in enriched precipitation δ^{18}O values in the PRB and adjacent regions (Figure 3).

3.3.2. Local Meteorological and Geographical Factors Controlling Spatial Precipitation $\delta^{18}O$ Variation. In order to explore the factors controlling spatial distribution of precipitation δ^{18}O in the PRB and adjacent regions, we compared the correlations between mean weighted precipitation δ^{18}O values and meteorological and geographical factors among stations, showing that mean values for atmospheric pressure, temperature, water vapor pressure, precipitation amount, and altitude show significant correlations with mean weighted precipitation δ^{18}O values in the annual time scale of the PRB and adjacent regions, with correlation coefficients of 0.929, 0.787, 0.786, 0.589, and −0.908, respectively, with P values < 0.01 for atmospheric pressure, temperature, water vapor pressure, altitude, and 0.05 for precipitation amount (Figures 6(a), 6(b), 6(c), 6(e), and 6(d)). This suggests that they are the main factors controlling spatial precipitation δ^{18}O variation. The slope of $d\delta^{18}O_p/dT$ and $d\delta^{18}O_p/dP$ is 0.34‰/°C (Figure 6(b)) and 1.7‰/100 mm (Figure 6(d)), respectively.

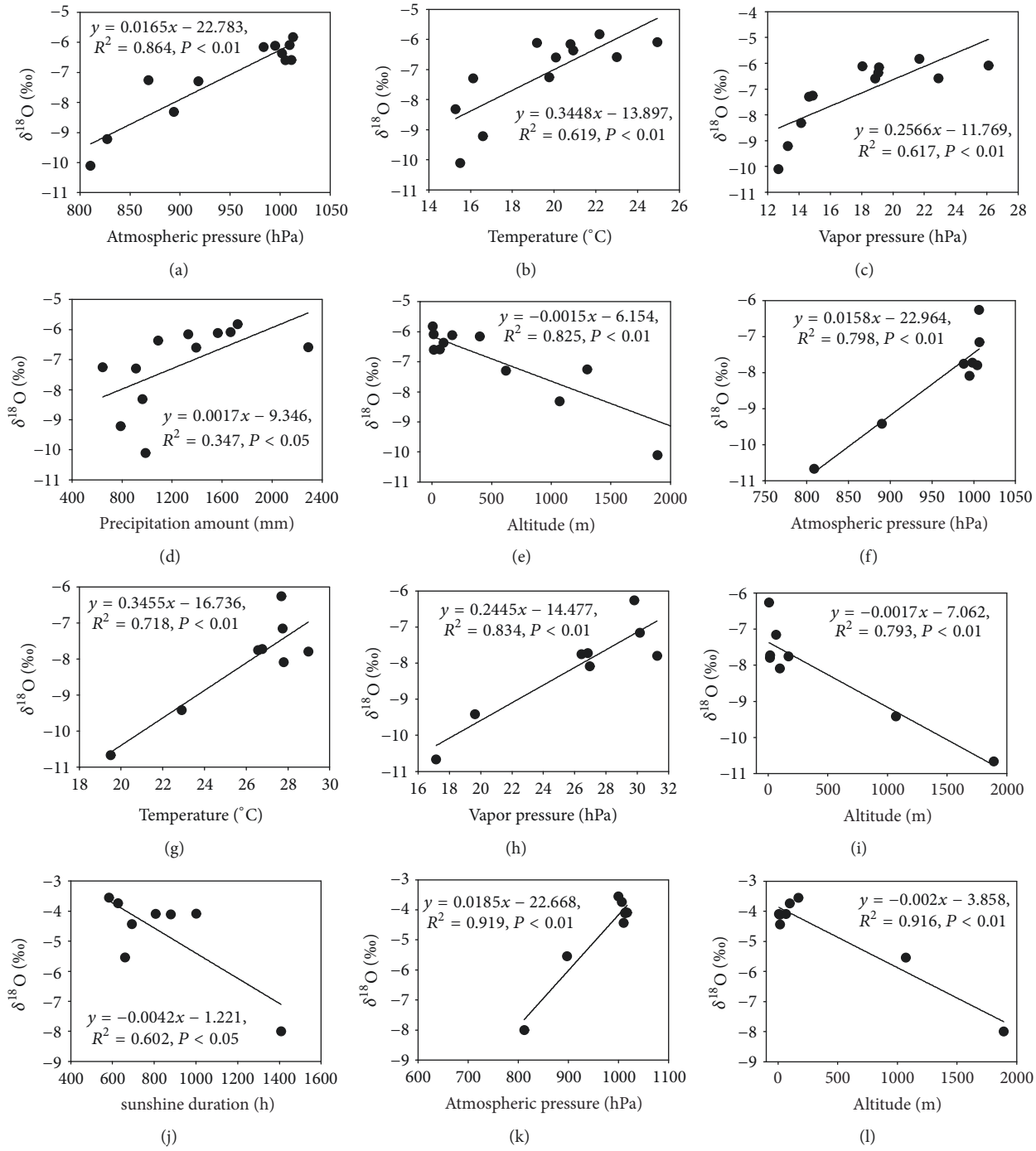

Figure 6: Correlations of mean weighted precipitation $\delta^{18}O$ values for stations with meteorological and geographical factors which are at P value < 0.05 or 0.01. Note: (a), (b), (c), (d), and (e) represent the mean annual values; (f), (g), (h), and (i) represent the mean values for the summer monsoon period; (j), (k), and (l) represent the mean values for the nonsummer monsoon period.

The slope of $d\delta^{18}O_p/dT$ is higher than the northeast regions of China (0.27‰/°C) and slightly lower than the northwest regions of China (0.37‰/°C) [21]. The slope of $d\delta^{18}O_p/d\text{ALT}$ is −0.15‰/100 m (Figure 6(e)), which indicates the "altitude effect" on the weighted mean annual precipitation $\delta^{18}O$ values, which is lower than that found for the Tibet Plateau (−0.3‰/100 m) by Liu et al. [21] and for the globe (−0.28‰/100 m) by Poage and Chamberlain [36]. However, this is similar to the whole country scale found for China (−0.15‰/100 m and −0.13‰/100 m) by Liu et al. [16] and Liu et al. [21], respectively.

In the summer monsoon period, the controlling factors for spatial precipitation $\delta^{18}O$ variation is atmospheric pressure, temperature, vapor pressure, and altitude, exhibiting

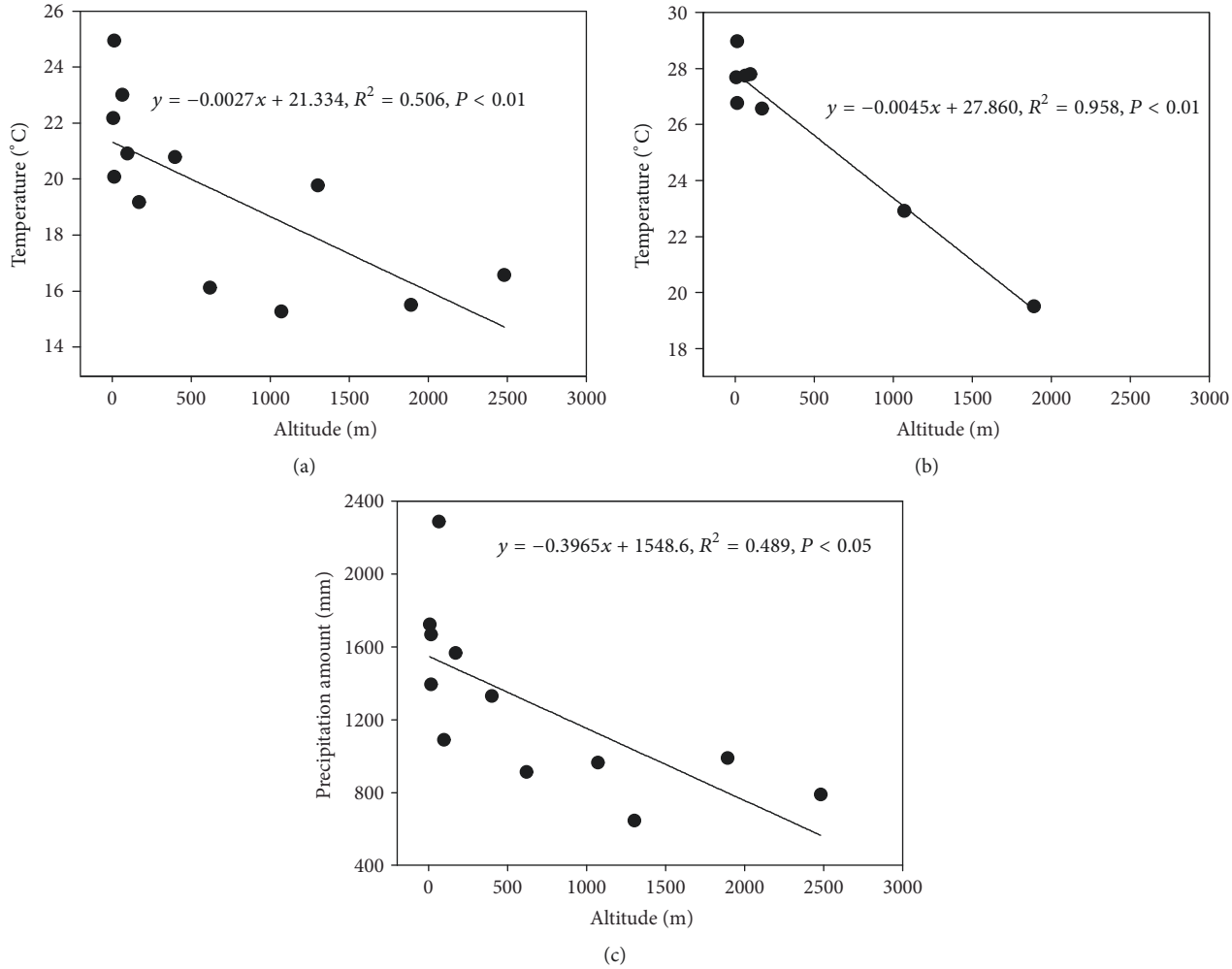

Figure 7: Correlations of mean annual temperature (a), mean summer monsoon temperature (b), and mean annual precipitation (c) for stations with altitude.

correlation coefficients of 0.930, 0.889, 0.913, and −0.921, respectively, with all the P values < 0.01 (Figures 6(f), 6(g), 6(h), and 6(i)). The slope of $d\delta^{18}O_p/dT$ and $d\delta^{18}O_p/d\text{ALT}$ is 0.35‰/°C (Figure 6(g)) and −0.17‰/100 m (Figure 6(i)), respectively, which is similar to that for the annual time scale.

In the nonsummer monsoon period, the controlling factors for the precipitation $\delta^{18}O$ values are sunshine duration, atmospheric pressure, and altitude, with correlation coefficients of −0.776, 0.959, and −0.957, respectively, explaining 60.2%, 91.9%, and 91.6% of the variance, respectively, with P values < 0.05, 0.01, and 0.01 (Figures 6(j), 6(k), and 6(l)). The $d\delta^{18}O_p/d\text{ALT}$ is −0.20‰/100 m (Figure 6(l)), suggesting that the "altitude effect" for the nonsummer monsoon period is the most significant among the three time periods.

However, mean temperature shows significantly positive correlation with mean weighted precipitation $\delta^{18}O$ in the annual time scale and the summer monsoon period (Figures 6(b) and 6(g)). Meanwhile, mean precipitation also shows significantly positive correlation with mean weighted precipitation $\delta^{18}O$ values (Figure 6(d)). Moreover, both temperature and precipitation show significantly negative correlations with altitude (Figure 7). This indicates that the correlations of precipitation and temperature may reflect the result of the "altitude effect," suggesting that altitude should be the more significant factor for spatial precipitation $\delta^{18}O$ variation in the PRB and adjacent regions.

3.4. Simulation of Precipitation $\delta^{18}O$ in the PRB and Adjacent Regions

3.4.1. Nonlinear Regression Model and Linear Regression Model. The Bowen and Wilkinson model has been applied widely for simulating the precipitation $\delta^{18}O$ in monsoon climatic zones [3, 10, 16]. No significant interaction effect of latitude and altitude has been found since the stations are mostly situated below 200 m [14]. The interaction effect of latitude and altitude occurs when stations are both below 200 m and above 200 m [16], and the elevation of our research area ranges from 0 to 2852 m. Therefore, we adopt a nonlinear fit to consider the correlation between latitude (LAT) and altitude (ALT) to establish the mean weighted precipitation $\delta^{18}O$ patterns under the three time scales: the annual time scale,

summer monsoon, and nonsummer monsoon periods. The model equations are as follows:

$$\delta^{18}O = -0.062LAT^2 + 2.792LAT - 0.001ALT - 37.251 \quad (5)$$

$$\delta^{18}O = -0.072LAT^2 + 3.315LAT - 0.002ALT - 45.091 \quad (6)$$

$$\delta^{18}O = -0.007LAT^2 + 3.383LAT - 0.002ALT - 9.056, \quad (7)$$

where (5), (6), and (7) represent the mean weighted precipitation $\delta^{18}O$ patterns for the annual time scale, summer monsoon, and nonsummer monsoon periods, respectively.

According to the above results (Figure 6), we establish linear regression models using those meteorological and geographical variables for modeling in the three time periods. The resulting models are as follows:

$$\delta^{18}O = 0.015AP + 0.271T - 0.173VP - 0.0006P - 0.0004ALT - 22.429 \quad (8)$$

$$\delta^{18}O = 0.034AP - 0.646T + 0.222VP + 0.0004ALT - 30.177 \quad (9)$$

$$\delta^{18}O = -0.002S + 0.098AP + 0.009ALT - 101.567, \quad (10)$$

where (8), (9), and (10) represent the mean weighted precipitation $\delta^{18}O$ patterns for the annual time scale, summer monsoon, and nonsummer monsoon periods, respectively. The parameters, S, VP, T, AP, P, and ALT represent sunshine duration (h), vapor pressure (hPa), air temperature (°C), atmospheric pressure (hPa), precipitation amount (mm), and altitude (m), respectively.

By comparing the results of the Bowen and Wilkinson model with other researches, the regression coefficients of the second-order term (−0.062) (see (5)) are significantly more negative than that modeled on a global scale (−0.0051) [14] or modeled for the United States (−0.0057) [37] and China (−0.0073) [16]. This may be caused by the smallest area of our study. And the PRB and adjacent regions are significantly influenced by both the southeast and southwest monsoons, and precipitation $\delta^{18}O$ depleted as moisture is transferred from the oceans to the PRB and adjacent regions. Moreover, the Bowen and Wilkinson model estimates the best precipitation $\delta^{18}O$ patterns for nonsummer monsoon period (Figure 8). Zhao et al. [3] found that the Bowen and Wilkinson model could estimate precipitation $\delta^{18}O$ well only in winter for China. This suggests that there are differences in modeling the precipitation $\delta^{18}O$ by the Bowen and Wilkinson model for different regional scales and time scales in the monsoon climatic regions.

By comparing the results of the Bowen and Wilkinson model with the linear regression model, the results show that the linear regression model also estimates the best precipitation $\delta^{18}O$ patterns for the nonsummer monsoon period (Figure 8). The amount of variance explained by the linear regression model is higher (93.5%, 92.8%, and 99.0%, resp.) than those (85.8%, 90%, and 92.4%, resp.) (Figure 8) by the Bowen and Wilkinson model for the annual time scale, summer monsoon, and nonsummer monsoon periods, respectively. Moreover, the mean errors explained by the linear regression model are lower (0.27‰ and 0.24‰, resp.) than those (0.48‰ and 0.35‰, resp.) by the Bowen and Wilkinson model for the annual time scale and the summer monsoon period. There is a higher mean error (0.41‰) in the linear regression model than that in the Bowen and Wilkinson model (0.32‰) for the nonsummer monsoon period, but the linear regression model explains more variance with a lower standard deviation of mean error (99.0‰ and 0.19‰, resp.) than does the Bowen and Wilkinson model (92.4‰ and 0.22‰, resp.). The results suggest that precipitation $\delta^{18}O$ can be estimated more accurately by the linear regression model than by the Bowen and Wilkinson model in the PRB and adjacent regions.

3.5. Spatial Distribution of Precipitation $\delta^{18}O$ in the PRB. Spatial distribution of precipitation $\delta^{18}O$ values from 1980 to 2011 for the annual time scale, summer monsoon, and nonsummer monsoon periods of the PRB are presented based on (8), (9), and (10), respectively. The data utilized come from the meteorological data network of China (Figure 9(a)). Precipitation $\delta^{18}O$ values are gradually more depleted (Figure 9) from the south and east to the north and northwest, especially in the annual time scale and the summer monsoon period, which are mainly caused by "altitude effect." Precipitation $\delta^{18}O$ values are more depleted in the summer monsoon period and more enriched in the nonsummer monsoon period (Figures 9(c) and 9(d)). However, spatial distribution of precipitation $\delta^{18}O$ reflect only the results of the linear regression model based on limited quantities and years of observation stations. As a result, more of the long-time observation stations should be established for more accurate estimation of precipitation $\delta^{18}O$ variations in the monsoon climatic regions.

4. Conclusions

Based on the precipitation $\delta^{18}O$ values from the datasets of the Global Network of Isotopes in Precipitation (GNIP), the National Centers for Environmental Prediction/National Center for Atmospheric Research (NCEP/NCAR) Reanalysis data, and previous researches, we explored the temporal and spatial variations of precipitation $\delta^{18}O$ in the PRB and adjacent regions. The principal conclusions are as follows:

(1) There was no "temperature effect" for the precipitation $\delta^{18}O$ for each station in the PRB and adjacent regions. "Amount effect" has been found at all stations (except for Haikou) for the annual time scale, while only three stations show the "amount effect" in the summer monsoon and nonsummer monsoon periods.

(2) Temporal variations show that the most depleted mean monthly precipitation $\delta^{18}O$ value does not occur in the month with the most mean monthly precipitation amount, which should be correlated

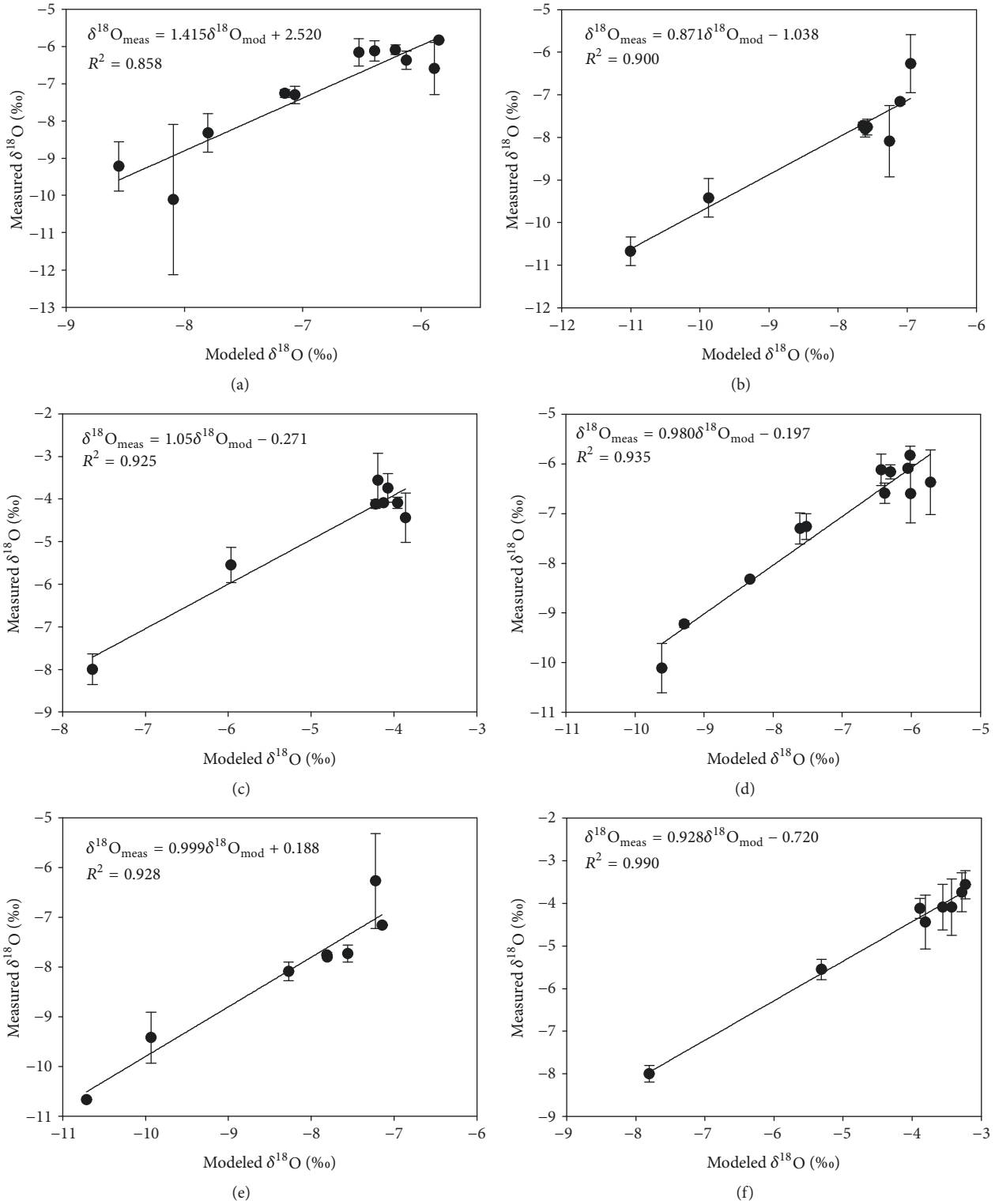

Figure 8: Linear correlations between measured amount-weighted precipitation $\delta^{18}O$ and modeled weighted precipitation $\delta^{18}O$. Note: (a), (b), and (c) represent (5), (6), and (7) by the Bowen and Wilkinson model, respectively; (d), (e), and (f) represent (8), (9), and (10) by the linear regression model, respectively.

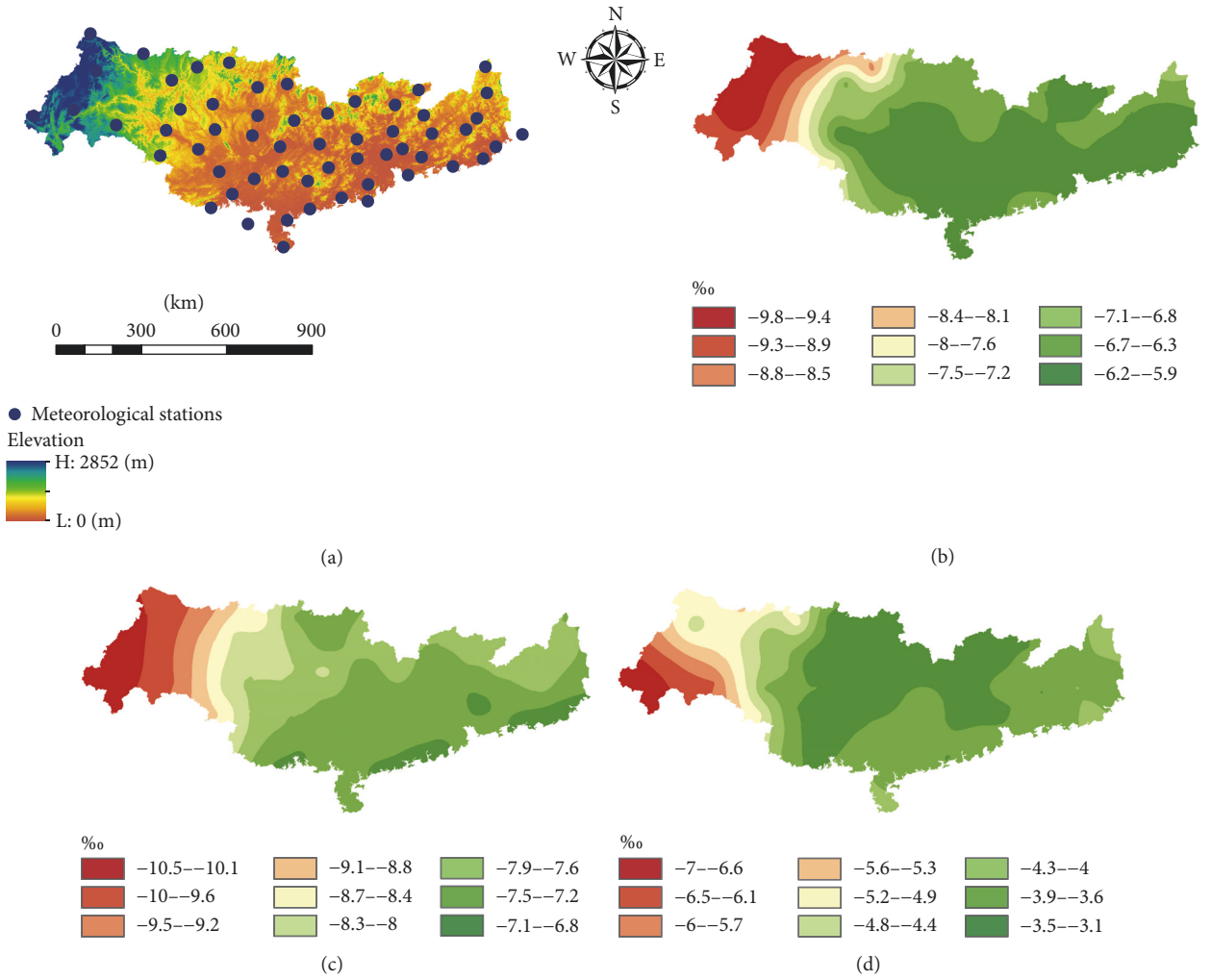

FIGURE 9: Spatial distribution of mean weighted precipitation $\delta^{18}O$ values over Pearl River basin of China based on the Kriging method from 1980 to 2011. Note: (a) represents meteorological stations in the Pearl River basin; (b) represents spatial distribution of the mean weighted annual precipitation $\delta^{18}O$ values by (8); (c) represents spatial distribution of mean weighted precipitation $\delta^{18}O$ values for the summer monsoon period by (9); (d) represents spatial distribution of mean weighted precipitation $\delta^{18}O$ values for the nonsummer monsoon period by (10).

with water vapor sources, the distance of water vapor transport, the changes in location, and intensity of the intertropical convergence zone (ITCZ). Spatial variations show that the most depleted mean precipitation $\delta^{18}O$ values does not occur in the station with the most mean precipitation amount for the annual time scale. Meanwhile, "altitude effect" has been significantly found among stations and precipitation $\delta^{18}O$ values among stations show close correlation with local meteorological conditions, which can account for the characteristics in the spatial variations. This indicates that water vapor sources and changes in location and intensity of the ITCZ, "altitude effect" as well as local meteorological conditions should be taken significantly into consideration when interpreting the temporal and spatial variations of precipitation $\delta^{18}O$ rather than "amount effect" in the PRB and adjacent regions.

(3) We established linear regression models combining multiple meteorological variables for estimating the mean weighted precipitation $\delta^{18}O$ in the PRB for the annual time scale, summer monsoon, and nonsummer monsoon periods. The amounts of variances explained by the linear regression model are all more than 92%, which are higher than those explained by the Bowen and Wilkinson model, suggesting that the linear regression models can estimate more accurately than the Bowen and Wilkinson model in the PRB and adjacent regions.

(4) This research can provide useful information for rebuilding temporal and spatial precipitation $\delta^{18}O$ in the monsoon climatic regions. Meanwhile, more of the long-time observation stations should be established for more accurate estimation of precipitation $\delta^{18}O$ variations in the monsoon climatic regions.

Conflicts of Interest

The authors declare that there are no conflicts of interest.

Acknowledgments

This research was supported by the National Natural Science Foundation of China (41371058, 4161101254, and 41561144012).

References

[1] K. Rozanski, L. Araguas-Araguas, and R. Gonfiantini, "Isotopic patterns in modern global precipitation," in *Climate Change in Continental Isotopic Records*, P. K. Swart, K. C. Lohmann, J. McKenzie, and S. Savin, Eds., American Geophysical Union, pp. 1–36, Washington, DC, USA, 1993.

[2] X. Zhang, J. Liu, L. Tian, Y. He, and T. Yao, "Variations of δ^{18}O in precipitation along vapor transport paths," *Advances in Atmospheric Sciences*, vol. 21, no. 4, pp. 562–572, 2004.

[3] L. Zhao, H. Xiao, M. Zhou et al., "Factors controlling spatial and seasonal distributions of precipitation δ^{18}O in China," *Hydrological Processes*, vol. 26, no. 1, pp. 143–152, 2012.

[4] N. Kurita, N. Yoshida, G. Inoue, and E. A. Chayanova, "Modern isotope climatology of Russia: A first assessment," *Journal of Geophysical Research: Atmospheres*, vol. 109, article D03102, 2004.

[5] D. Brown, J. Worden, and D. Noone, "Comparison of atmospheric hydrology over convective continental regions using water vapor isotope measurements from space," *Journal of Geophysical Research: Atmospheres*, vol. 113, no. 15, Article ID D15124, 2008.

[6] V. I. Zakharov, R. Imasu, K. G. Gribanov, G. Hoffmann, and J. Jouzel, "Latitudinal distribution of the deuterium to hydrogen ratio in the atmospheric water vapor retrieved from IMG/ADEOS data," *Geophysical Research Letters*, vol. 31, no. 12, Article ID L12104, 2004.

[7] I. Clark and P. Fritz, *Environmental Isotopes in Hydrogeology*, Lewis Publishers, New York, NY, USA, 1997.

[8] L. Araguás-Araguás, K. Froehlich, and K. Rozanski, "Stable isotope composition of precipitation over southeast Asia," *Journal of Geophysical Research: Atmospheres*, vol. 103, no. D22, Article ID 98JD02582, pp. 28721–28742, 1998.

[9] S. Sengupta and A. Sarkar, "Stable isotope evidence of dual (Arabian Sea and Bay of Bengal) vapour sources in monsoonal precipitation over north India," *Earth and Planetary Science Letters*, vol. 250, no. 3-4, pp. 511–521, 2006.

[10] X. Liu, Z. Rao, X. Zhang, W. Huang, J. Chen, and F. Chen, "Variations in the oxygen isotopic composition of precipitation in the Tianshan Mountains region and their significance for the Westerly circulation," *Journal of Geographical Sciences*, vol. 25, no. 7, pp. 801–816, 2015.

[11] W. Yu, T. Yao, S. Lewis et al., "Stable oxygen isotope differences between the areas to the north and south of Qinling Mountains in China reveal different moisture sources," *International Journal of Climatology*, vol. 34, no. 6, pp. 1760–1772, 2014.

[12] B.-L. Cui and X.-Y. Li, "Stable isotopes reveal sources of precipitation in the Qinghai Lake Basin of the northeastern Tibetan Plateau," *Science of the Total Environment*, vol. 527-528, pp. 26–37, 2015.

[13] M. Tan, "Circulation effect: response of precipitation δ^{18}O to the ENSO cycle in monsoon regions of China," *Climate Dynamics*, vol. 42, no. 3-4, pp. 1067–1077, 2014.

[14] G. J. Bowen and B. Wilkinson, "Spatial distribution of δ^{18}O in meteoric precipitation," *Geology*, vol. 30, no. 4, pp. 315–318, 2002.

[15] J. Liu, X. Song, G. Yuan et al., "Stable isotopes of summer monsoonal precipitation in southern China and the moisture sources evidence from δ^{18}O signature," *Journal of Geographical Sciences*, vol. 18, no. 2, pp. 155–165, 2008.

[16] Z. Liu, L. Tian, X. Chai, and T. Yao, "A model-based determination of spatial variation of precipitation δ^{18}O over China," *Chemical Geology*, vol. 249, no. 1-2, pp. 203–212, 2008.

[17] T.-R. Peng, C.-H. Wang, C.-C. Huang, L.-Y. Fei, C.-T. A. Chen, and J.-L. Hwong, "Stable isotopic characteristic of Taiwan's precipitation: A case study of western Pacific monsoon region," *Earth and Planetary Science Letters*, vol. 289, no. 3-4, pp. 357–366, 2010.

[18] Y. Tang, H. Pang, W. Zhang, Y. Li, S. Wu, and S. Hou, "Effects of changes in moisture source and the upstream rainout on stable isotopes in precipitation -a case study in Nanjing, eastern China," *Hydrology and Earth System Sciences*, vol. 19, no. 10, pp. 4293–4306, 2015.

[19] L. Tian, T. Yao, K. MacClune et al., "Stable isotopic variations in west China: A consideration of moisture sources," *Journal of Geophysical Research: Atmospheres*, vol. 112, no. 10, Article ID D10112, 2007.

[20] X. P. Zhang, J. M. Liu, W. Z. Sun, Y. M. Huang, and J. M. Zhang, "Relations between oxygen stable isotopic ratios in precipitation and relevant meteorological factors in southwest China," *Science China Earth Sciences*, vol. 50, no. 4, pp. 571–581, 2007.

[21] J. Liu, X. Song, G. Yuan, X. Sun, and L. Yang, "Stable isotopic compositions of precipitation in China," *Tellus B: Chemical and Physical Meteorology*, vol. 66, no. 1, Article ID 22567, 2014.

[22] J. Wu, Y. Ding, B. Ye, Q. Yang, X. Zhang, and J. Wang, "Spatio-temporal variation of stable isotopes in precipitation in the Heihe River Basin, Northwestern China," *Environmental Earth Sciences*, vol. 61, no. 6, pp. 1123–1134, 2010.

[23] X. F. Li, M. J. Zhang, S. J. Wang, X. N. Ma, and F. Li, "Spatial and temporal variations of hydrogen and oxygen isotopes in precipitation in the yellow river basin and its environmental significance," *Acta Geologica Sinica*, vol. 87, no. 2, pp. 269–277, 2013 (Chinese).

[24] S. G. Pang, S. K. Zhao, R. Wen, and Z. F. Liu, "Spatial and temporal variation of stable isotopes in precipitation in the Haihe River basin," *Chinese Science Bulletin*, vol. 60, no. 13, pp. 1218–1226, 2015 (Chinese).

[25] J. B. Xue, W. Zhong, and Y. J. Zhao, "Stable oxygen isotope in precipitation in Guangzhou in relation to the meteorological factors and the monsoon activity," *Journal of Glaciology and Geocryology*, vol. 30, no. 5, pp. 761–768, 2008 (Chinese).

[26] Y. M. Huang, X. P. Zhang, X. Sun, Y. B. Huang, and N. Q. Wei, "Seasonal variations of stable isotope in precipitation and atmospheric water vapor and their relationship with moisture transportation in Changsha city," *Scientia Geographica Sinica*, vol. 35, no. 4, pp. 498–506, 2015 (Chinese).

[27] W. J. Luo and S. J. Wang, "Signal transmission of δ^{18}O in precipitation, soil water and dropping water of Liang Feng cave and its implications," *Chinese Science Bulletin*, vol. 53, no. 17, pp. 2071–2076, 2008 (Chinese).

[28] X. Wu, X. Y. Zhu, M. L. Zhang, X. Bai, and B. Y. Zhang, "High-resolution stable isotope record of atmospheric precipitation,"

Resources and Environment in the Yangtze Basin, vol. 22, no. 2, pp. 182–188, 2013 (Chinese).

[29] T. B. Coplen, "Reporting of stable carbon, hydrogen and oxygen abundances," IAEA Tecdoc 825, International Atomic Energy Agency, Vienna, Austria, 1995.

[30] G. Li, X. P. Zhang, H. W. Wu, J. M. Zhang, N. Q. Wei, and H. Huang, "Stable oxygen isotope in precipitation in relation to the meteorological factors and the moisture sources in Yunnan," *Journal of Natural Resources*, vol. 29, no. 6, pp. 1043–1052, 2014 (Chinese).

[31] M. Vuille, M. Werner, R. S. Bradley, and F. Keimig, "Stable isotopes in precipitation in the Asian monsoon region," *Journal of Geophysical Research: Atmospheres*, vol. 110, no. 23, Article ID D23108, pp. 1–15, 2005.

[32] W. Dansgaard, "Stable isotopes in precipitation," *Tellus*, vol. 16, no. 4, pp. 436–468, 1964.

[33] S. K. Bhattacharya, K. Froehlich, P. K. Aggarwal, and K. M. Kulkarni, "Isotopic variation in indian monsoon precipitation: records from bombay and new delhi," *Geophysical Research Letters*, vol. 30, no. 24, pp. 2285–2289, 2003.

[34] S. F. M. Breitenbach, J. F. Adkins, H. Meyer, N. Marwan, K. K. Kumar, and G. H. Haug, "Strong influence of water vapor source dynamics on stable isotopes in precipitation observed in Southern Meghalaya, NE India," *Earth and Planetary Science Letters*, vol. 292, no. 1-2, pp. 212–220, 2010.

[35] K. D. Prasad and S. D. Bansod, "Interannual variations of outgoing longwave radiation and Indian summer monsoon rainfall," *International Journal of Climatology*, vol. 20, no. 15, pp. 1955–1964, 2000.

[36] M. A. Poage and C. P. Chamberlain, "Empirical relationships between elevation and the stable isotope composition of precipitation and surface waters: Considerations for studies of paleoelevation change," *American Journal of Science*, vol. 301, no. 1, pp. 1–15, 2001.

[37] A. Dutton, B. H. Wilkinson, J. M. Welker, G. J. Bowen, and K. C. Lohmann, "Spatial distribution and seasonal variation in $^{18}O/^{16}O$ of modern precipitation and river water across the conterminous USA," *Hydrological Processes*, vol. 19, no. 20, pp. 4121–4146, 2005.